

New Resolution Independent Measures of Circularity

Nicola Ritter · James Cooper

Published online: 29 May 2009
© Springer Science+Business Media, LLC 2009

Abstract In this paper we demonstrate that the most commonly used mathematical measure of circularity—the Form Factor—is highly resolution dependent. Furthermore we show that despite the abundance of papers proposing measures of roundness, most of the new measures are mathematically equivalent to the Form Factor. Only four measures were found that were different. We then present two new measures, the first based on the theory of Mean Deviations and the second based on the mathematical definition of a circle. When compared in terms of resolution dependence, order of complexity, ease of calculation, and how well they match human perception, the two new measures are shown to be better overall than the previous measures. The two new measures are resolution independent in the sense that changing the resolution makes no change to the order of circularity of different shapes. That is, changing the resolution does not change whether one object would be considered more round than another on the basis of the measure. None of the other measures has this property.

Keywords Circularity · Roundness · Shape · Resolution · Human perception

1 Introduction

The measuring of roundness has widespread application in such diverse fields as biology [1–9]; medicine [10–15]; in-

dustrial processing [16–20]; botany [21, 22]; geology [23]; dentistry [24]; paleontology [25]; and physics [26].

In all fields similar questions are posed: “is an object round?”, “is it more round than another object?”, “can its roundness be used for classification purposes?”. To this end various calculations have been proposed that measure roundness, however many of these are actually mathematical derivations of each other. Furthermore there has been little research comparing these measures with each other or comparing them under different resolutions.

This paper reviews previously presented measures of roundness in Sect. 2. We then present two new measures of roundness in Sect. 3. Comparisons between the various measures are then presented in Sect. 4. Section 5 presents the conclusions of these comparisons.

2 Review of Circularity Measures

2.1 Area-Perimeter Comparison

The most commonly used measure of roundness is that described by Cox [27] in 1927 which he calls ‘percentage roundness’, despite the fact that it is not actually a percentage. Since then this measure has been used by many researchers [4–9, 12, 13, 15, 17, 18, 25, 28–31] and given many different names. We choose to call it the Form Factor in line with the American Society for Testing and Materials [32].

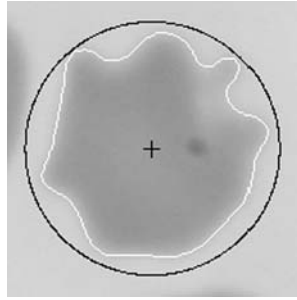
The Form Factor is best described as the ratio of the area of the object to the area of a circle with the same perimeter as the object. However it is usually calculated using the perimeter itself:

$$FF = \frac{A}{A_p} = \frac{4\pi A}{P^2}, \quad (1)$$

N. Ritter (✉)
Murdoch University, Perth, Western Australia, Australia
e-mail: nritter@lynx.com.au

J. Cooper
Curtin University, Bentley, Australia

Fig. 1 The Form Factor is the ratio of the area of an object to the area of a circle with the same perimeter as the object



where A is the area of the object, A_p is the area of a circle with the same perimeter as the object and P is the object's perimeter. The Form Factor for all objects lies in the range $(0, 1]$, with only a circle giving the highest value of 1. A diagram illustrating the meaning of this measure can be seen in Fig. 1.

Derivations of this measure are also proposed in the literature, often described as if they were new measures. Richardson [33] defines 'homoplaty' as

$$H = \frac{2\sqrt{\pi A}}{P}. \quad (2)$$

However, this is the square root of the Form Factor defined in (1). The additional square root calculation adds no more than a nonlinear scaling of the Form Factor at the cost of the function call.

Foresto, D'Arrigo, Carreras, Cuezco, Valverde and Rasia [8] define the 'aggregate shape factor' as

$$ASP = \frac{A}{P^2}. \quad (3)$$

This measure is a non-normalised version of the Form Factor. In effect this means that its range is $(0, 4\pi]$, which is a less intuitive range than the normalised version.

Hausner [34] defines 'surface factor' as

$$SF = \frac{P^2}{4\pi A}, \quad (4)$$

and this inverse of the Form Factor is also used by others [19, 22, 24, 35]. This measure has the disadvantage that its range is in fact $[1, \infty)$, where a circle has value 1. Therefore the surface factor is a measure of non-roundness rather than roundness, making its inverse—the Form Factor—a preferable measure of circularity. A non-normalised version of the inverse has also been used [1–3, 6, 21, 26]. Gordon, Colman-Lerner, Chin, Benjamin, Yu and Brent [15] subtract 1 from the inverse to give a range of $[0, \infty)$.

Moschakis, Murray and Dickinson [20] divide the inverse of the Form Factor by 1.064 to compensate for the square corners produced by digitisation:

$$R_{MMD} = \frac{P^2}{4\pi A 1.064}. \quad (5)$$

However, this linear scaling adds little utility to the inverse form factor, as it does not change the relative values for different objects.

Diamond, Berry, Jewett, Eggleston and Coffey [36] define a 'new' measure they call the 'nuclear roundness factor':

$$NRF = \frac{r_p}{r_a}, \quad (6)$$

where r_p is the radius of a circle with the same perimeter as the object, and r_a is the radius of a circle with the same area. However it can be shown that

$$NRF = \sqrt{\frac{1}{FF}}. \quad (7)$$

Therefore this proposed measure is in fact the inverse square root of the Form Factor.

As stated previously, the Form Factor and its mathematical derivations have been widely used. However in 1961 Richardson [33] mentioned—and later Mandelbrot [37] showed—that the perimeter of a shape increases as the unit of measure decreases. Increasing the resolution of an image is equivalent to reducing the unit of measure, and hence one could expect the perimeter to grow non-linearly with increased resolution. This means that the Form Factor is probably resolution dependent [30].

A second problem with the Form Factor is the difficulty of calculating the perimeter of digitised images per se [38]. In fact the Form Factor was originally designed as a non-discrete measure and it has been demonstrated that it is more accurately defined as a measure of octagonality [39] when used on digitised images. Calculation of the perimeter is covered in more detail in Sect. 4.2.

2.2 Methods That Use Sampling

In an attempt to solve the two problems—resolution dependence and perimeter inaccuracy—Hawkins [40] defines a 'projection shape factor'—which we shall call the Sampled Form Factor—which uses an estimate of perimeter taken from multiple radii:

$$SFF = \frac{4\pi A}{P_5^2}, \quad (8)$$

where P_5 is the length of connected edge pixels at 5-degree intervals. In essence the area is being compared with a smoothed border.

Gordon et al. [15], also use a sampling method. The lengths of 128 radii at evenly spaced angles around the object are transformed using the Discrete Fourier Transform (DFT). For circular objects $DFT(0)$ will be non-zero and $DFT(\omega)$, $\omega > 0$ will be zero. For all other objects $DFT(\omega)$,

Fig. 2 Finding perimeter points or radii lengths at regular degree intervals is undefined for some objects

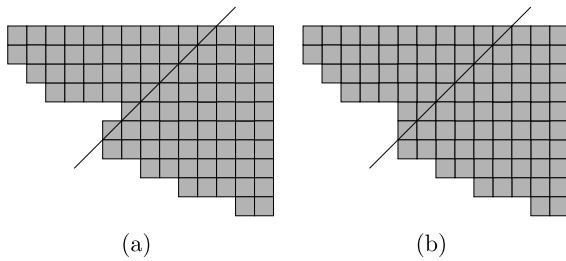
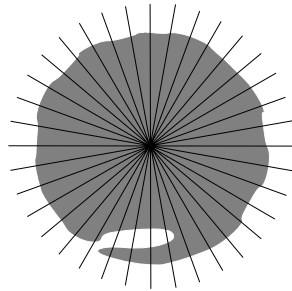


Fig. 3 Parts of two objects. The one pixel difference means that the object on the left will have multiple border points along the radial sampling line and so could not be used by radial sampling methods, whereas the object on the right could be used

$\omega > 0$ will be positive. Fourier Transform Roundness can therefore be defined as

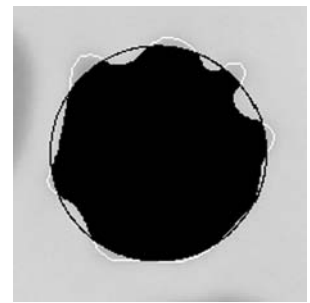
$$FTR = \sqrt{\sum_{\omega > 0} \left| \frac{DFT(\omega)}{DFT(0)} \right|^2}. \tag{9}$$

This measure gives a value of 0 for a circle, with increasing values for increasingly irregular objects.

However there are problems with measures that do sampling in the manner described in these two papers, because selection of the points is undefined for objects that have more than one border point on any particular trajectory from the centre. An example of such a shape is shown in Fig. 2.

Hawkins does not propose a solution to this problem, however Gordon et al. address the problem by setting the value of *FTR* to -1 in such situations, which was a successful solution in their domain. However, problems may occur when a small irregularity in the border—such as that shown in Fig. 3(a)—leads to the inability to calculate a value for an object which may be close to circular. This problem may also become more likely with higher resolutions. Furthermore, a one-pixel difference in the border of the object—such as that in Fig. 3(b)—would change the result of the calculation. For these reasons, methods that use sampling might only be useful in a limited set of situations and not generally viable solutions for calculating roundness.

Fig. 4 The Circularity Factor is the ratio of the area of intersection of an object with a circle with same area and centre as the object, to the area of the object itself. In the diagram above it is the ratio of the number of black pixels to the number of pixels enclosed in and inclusive of the object border



2.3 Area-Area Comparison

Giger, Doi and MacMahon [11] define a measure that they call circularity, but which we will call the Circularity Factor, to avoid confusion with the generic term circularity. This measure is defined as:

$$CF = \frac{|A \cap D|}{|A|}, \tag{10}$$

where *A* is the set of pixels defining object *A* and *D* is the set of pixels defining a discrete disk centred on the centre of gravity of object *A* and with the same area as *A*. A diagram illustrating the meaning of this measure can be seen in Fig. 4. A discrete circle centred on the exact centre of an object will not necessarily have the exact area of the object, therefore Bottema [39] suggested that it would be better to search for a nearby centre that *does* allow a disk with the exact area. However the difference in the areas is only significant for very small objects or objects at very low resolution and there is a time cost in searching for such a perfect discrete disk.

2.4 Area-Diameter Comparison

Pentland [41]—also in 1927—defines a measure he calls ‘projection sphericity’ which others [13, 17, 32] have called ‘roundness’. We will call this measure the ‘Roundness Factor’ to save confusion with the generic term ‘roundness’. This measure compares the area of the object with the area of a circle that has the same maximum diameter of the object. A diagram illustrating this measure can be seen in Fig. 5. As with the Form Factor, the definition using area is more easily calculated by conversion to more measurable values:

$$RF = \frac{A}{A_{dmax}} = \frac{4A}{\pi d_{max}^2}, \tag{11}$$

where A_{dmax} is the area of a circle with the same maximum diameter as the object, and d_{max} is the maximum diameter, defined as the length of the longest line that can be drawn between two points on the border of the object (see Fig. 5). Like the Form Factor this measure has a value of 1 for a circle and a range of (0, 1].

Fig. 5 The Roundness Factor is the ratio of the area of an object to the area of the circle with a diameter equal to the longest diameter of the object

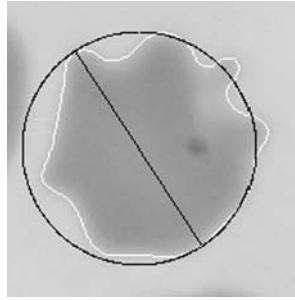
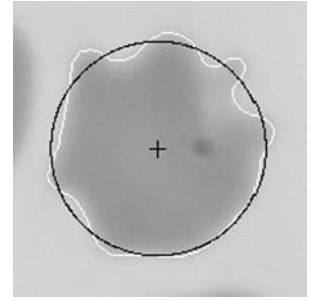


Fig. 6 The Mean Deviation is the sum of the absolute difference between the radius of each border pixel and the average radius



2.5 Mean Deviations

The traditional way of measuring deviation from a desired form is with a mean deviation. The mean deviation for a circle would therefore be defined as

$$MD = \frac{1}{n} \sum_{i=1}^n |r_i - \bar{r}_g|, \quad (12)$$

where n is the number of points on the perimeter, r_i is the radius at perimeter point i —measured relative to the centre of gravity of the object—and \bar{r}_g is the average radius, again relative to the centre of gravity. This is illustrated in Fig. 6, which shows the circle of average radius, to which the border points are compared for this circularity method. The main disadvantage of this method is that the deviations are size dependent, making the method size dependent.

For this reason Almeida-Prieto, Blanco-Mendez and Otero-Espinar [18] develop a measure based on the Mean Deviation, that they call the ‘mean percentage deviation’ of radius:

$$MPDR = \frac{100}{n} \sum_{i=1}^n \frac{|r_i - \bar{r}_g|}{\bar{r}_g}, \quad (13)$$

which is a normalised version of the mean deviation multiplied by 100 to give it a semblance of a percentage. This measure solves the size dependency of other mean deviation measures, however it still has several disadvantages. Firstly it is a measure of non-roundness rather than roundness. Secondly—despite its name—it is not a percentage. In fact its upper bound is difficult to determine mathematically. However if one considers a straight line to be the least circular of objects then it can be shown that as line length n increases the MPDR tends towards 50 rather than 100. In the next section we give a measure based on the Mean Deviation that removes these disadvantages.

3 Two New Measures of Roundness

3.1 Mean Roundness

The disadvantages of the Mean Percentage Deviation can be solved by developing an inverse measure based on the Mean Deviation (12). We therefore define the *Mean Roundness* as

$$MR = \frac{1}{n} \sum_{j=1}^n \frac{\bar{r}_b}{|r_j - \bar{r}_b| + \bar{r}_b}, \quad (14)$$

where \bar{r}_b is the average radius from the border points to the centre of the border—defined in Sect. 4.2—and r_j is the radius of border point j relative to the centre of the border. We use the centre of the border rather than the centre of gravity as it is much faster to calculate than the centre of gravity and requires only knowledge of the border points.

3.2 The Radius Ratio

By definition a circle is a shape in which all radii are the same length. We therefore posit that an examination of only the longest and shortest radii can be successfully used as a measure of roundness.

We therefore define the *Radius Ratio* as

$$RR = \frac{r_{bmin}}{r_{bmax}}, \quad (15)$$

where r_{bmin} is the minimum radius of a border point from the centre of the border, and r_{bmax} is the maximum radius.

4 Comparison of Measures

4.1 Criteria for Comparison

To enable a comparison between measures it is necessary to have a set of criteria that defines ‘best’. We therefore define the ideal measure of roundness as having the following attributes:

1. It should be resolution independent. That is, the threshold used to discriminate circular from non-circular shapes should be the same for any resolution, so that the measure becomes independent of the equipment.
2. It should be consistent. That is, the ordering of objects by the measure should be the same at any resolution.
3. It should be efficient to calculate, preferably with $O(n)$ complexity.
4. It should be defined for all two-dimensional objects.
5. The results should match those of human perception.
6. It should be a measure of ‘roundness’, rather than ‘non-roundness’—that is its value should be higher the more circular the shape—with a range of $(0, 1]$, where 1 is scored only by a perfect circle. Note, however, that no measure need be rejected based on this alone, as a new measure that fits this criteria can always be developed from the original measure.

Five of the measures to be compared—the Form Factor (1), the Roundness Factor (11), the Circularity Factor (10), the Mean Roundness (14) and the Radius Ratio (15)—conform to attributes 4 and 6 above.

The Fourier Transform Roundness (16) does not conform to attribute 6, however we found empirically that it has a range of $[0, 1)$, where a circle has a value of 0. We therefore define the Fourier Transform Circularity (FTC) as:

$$FTC = 1 - FTR, \tag{16}$$

this gives a range of $(0..1]$ as for the others.

Both the methods using sampling—the Sampled Form Factor (8) and the FTC (16)—theoretically fail to satisfy the requirement that the measure be defined for all two dimensional shapes. However, we have included them in our analysis, so as to find out how often they fail in practice. When they fail to calculate a value they will return -1 , allowing identification of such cases.

In terms of ease of calculation, the Radius Ratio, Mean Roundness and Fourier Transform Circularity only require the border to be identified, whereas the Circularity Factor requires identification of the points comprising the object itself, and the Form Factor, Sampled Form Factor and Roundness Factor require both the border and the object points.

The Circularity Factor has complexity $O(m)$ where m is the number of points comprising the object. The Roundness

factor and Fourier Transform Circularity both have complexity of $O(n \log n)$ —where n is the number of points in the border. The Mean Roundness, Form Factor, Sampled Form Factor and Radius Ratio have complexity of $O(n)$. However it should be noted that the Mean Roundness requires each border point to be visited twice: firstly to calculate the mean radius and secondly to calculate the mean difference. Since the other three methods with complexity $O(n)$ only require one loop, they may be faster to calculate.

4.2 Image Measurements

The following measurements were used when calculating the measures to be compared.

The border of an object is defined as an ordered one-pixel-width, 8-connected sequence of n pixels. It is represented by a vector of pixels b_1, b_2, \dots, b_n where each pixel touches the previous pixel at either a corner or along an edge. All pixels inside the border belong to the object, all pixels outside the border do not.

The perimeter of an object is calculated using

$$P = \sum_{i=1}^{n-1} D(b_i, b_{i+1}), \tag{17}$$

where b_i is a point in the border vector and D is given by

$$D = \begin{cases} 0.948 & \text{where } b_i \text{ and } b_{i+1} \text{ are horizontally} \\ & \text{or vertically adjacent} \\ 1.343 & \text{where } b_i \text{ and } b_{i+1} \text{ are diagonal} \\ & \text{to each other.} \end{cases} \tag{18}$$

These values seem counter-intuitive to the accepted values of 1 and $\sqrt{2}$, however they are shown by Dorst and Smeulders [38] to be on average more accurate. We confirm this, finding that for shapes for which it was possible to calculate the perimeter mathematically based on the length of one edge—for example the circle, square and octagon—the maximum inaccuracy dropped from 8.1% to 5.5%.

Since the perimeter is measured passing through the centres of the pixels that form the border, it effectively cuts each border point in two. Therefore the area is calculated as:

$$A = m + 0.5n, \tag{19}$$

where m is the number of points inside the border. It is worth noting that this formula was found to have inaccuracy of less than 1% for all shapes for which it was feasible to calculate the area mathematically.

The centre of the border is calculated as

$$C_b = \frac{1}{n} \sum_{i=1}^n b_i. \tag{20}$$

The centre of gravity is similarly calculated as

$$C_g = \frac{1}{m+n} \left(\sum_{j=1}^m o_j + \sum_{i=1}^n b_i \right), \quad (21)$$

where o_i is a point internal to the object.

The maximum diameter is calculated using the ‘rotating caliper’ method [42] on the convex hull, which is found using the ‘Graham Scan’ algorithm [43].

The intersection of an object pixel and the discrete disk of the same area is, of course, dependent on the algorithm used to draw the ‘circle’ that forms the discrete disk. For ease of calculation, we are assuming that an object pixel intersects with the discrete disk if its centre falls within the radius of the disk.

For the methods that use sampling, the shape was rejected if two or more border pixels lay on the same radial line from the border centre.

4.3 Basic Shapes

As a first step in considering the usefulness of the five measures, 18 basic shapes were drawn digitally. For each image the points comprising the object were found using thresholding, and the border found using graph processing theory [44].

The measurements described in Sect. 4.2 were then used to calculate values using the seven methods under consideration. The shape set and full results of this can be found in Appendix A.

From these results it can be seen that the Form Factor is not a good measure of roundness as it places the octagon and rounded square ahead of the circle, which is consistent with the theoretical work of Bottema [39]. The Roundness Factor may also be considered poor as it includes the two circles with inclusions within the top three most round. This might be considered useful in some cases if it were not for the fact that the circles with identical shaped extrusions have much lower Roundness Factor values, which is inconsistent. The Mean Roundness and Radius Ratio score the same five shapes as most round, varying only slightly in order. The Circularity Factor has the same top three as do the Mean Roundness and Radius Ratio, however it is noticeable that it gives the long pointed intrusion and extrusion higher circularity values than the shorter, wider intrusion and extrusion. This seems counter-intuitive. Both of the methods that use sampling reject 8 out of the 18 shapes. However those shapes for which they can calculate circularity are ordered in a similar manner to each other and to the Mean Roundness.

4.4 Threshold Resolution Independence

Six shapes were drawn on paper (Fig. 7) and then scanned in at resolutions of 100, 200, 300, 400, 600 and 800 dpi. As

can be seen from the detailed results given in Appendix B, only the Mean Roundness and the Radius Ratio were shown to be resolution independent in that the order of circularity of objects was maintained between resolutions, therefore allowing a single threshold value to be used to determine circularity at any resolution.

The other measures all proved to be resolution dependent in some manner. The FF, SFF, RF, and CF all result in different values for at least one object at different resolutions. The Form Factor is the least resolution independent as it scatters all but shape number 2 over the range of calculated values. The Sampled Form Factor and Roundness Factor have some scattering and the Circularity Factor has one object out of place. The Fourier Transform Circularity does not scatter the values for the resolutions, however both it and the Sampled Form Factor fail to calculate values for some objects at each of the lowest four resolutions, and all objects at the two highest resolutions. The most circular of the objects—shape 1—could only be given a value at the lowest resolution. It is also worth noting that the FTC is the only measure that gave a less circular value to shape 1 as compared to the slightly wobbly circle (shape 3).

4.5 Ordering Consistency

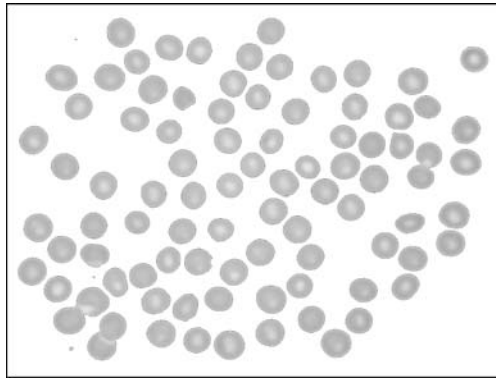
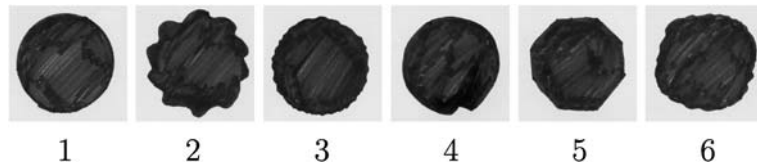
A second consideration is whether the order of the shapes is consistent *within* each resolution. That is, even if the threshold varies, the ordering of the objects by a measure should be the same no matter what the resolution. In other words whether *relative* roundness is consistent between the different resolutions.

In this respect the Form Factor, Sampled Form Factor, Roundness Factor and Circularity Factor all fail, with one or more differences in object order at different resolutions. The Fourier Transform Circularity was consistent, however it could not calculate values at high resolutions due to two or more points falling on a radial line. Both the Mean Roundness and Radius Ratio gave consistent ordering of objects for each resolution.

4.6 Human Perception Test Using Drawn Images

Since the Form Factor is highly resolution dependent, it cannot easily be compared to human perception of circularity for the six hand drawn images, therefore we do not discuss it here. For the Sampled Form Factor, Roundness Factor, Circularity Factor and Fourier Transform Circularity, the order used for comparison was the dominant one appearing in the results given in Appendix B.

The six shapes shown in Fig. 7 were given to 38 volunteers at a conference, who were asked to place them in order from most circular to least circular. 15 different combinations were chosen by the 38 people; all but 1 of the combinations (selected by only 1 person) had object 1 as the

Fig. 7 Six hand-drawn shapes**Fig. 8** One of the four images of red blood cells used for a human perception test. The images have been processed to remove the background, segment the objects, and identify the object borders

most circular. Analysing the combinations compared to the order of results of the four resolution independent measures showed that the Sampled Form Factor, Mean Roundness and Circularity Factor more closely matched human perception than did the Radius Ratio or the Fourier Transform Circularity. The best match of all was given by the Roundness Factor.

4.7 Human Perception Test Using Natural Images

To compare the measures with human perception of naturally formed shapes, four images of slides of red blood cells—an example is shown in Fig. 8—were segmented [44]. The images were then printed on A4 sized paper with each cell numbered. The images contain a total of 339 objects. The images were given to a group of 16 university students with each image evaluated by four different people. Each person was required to judge each cell as either circular, indeterminate or non-circular. A decision of non-circular was then given a score of 0, indeterminate a score of 1 and circular a score of 2. The four scores were added up, giving a total score of between 0 and 8 for each object.

In order to enable comparison of the four roundness measures with the judgements of human observers, any score above 6 was deemed to denote a circular cell. This equates to at least three of the four judges declaring the object circular, or two judges declaring it circular and the other two undecided. All cells with a score of 0 were classed as non-circular. Using these criteria, out of the 339 objects in the images, 21 were counted as circular, 119 as non-circular and the rest as indeterminate. Values were then calculated for

each object for each of the seven measures under consideration.

When deciding if an object is circular it is normal to choose a threshold for the measure being used. Objects with a value above this threshold are considered circular and below it are considered non-circular. For each potential threshold a count can be made of the number of cells that are above the threshold for the measure, but which were considered to be non-circular by the survey participants. These are false-positive results. Similarly a count can be made of the number of cells that are below the threshold, but which were considered to be circular by the survey participants. These are false-negatives. Summing the false-positives and false-negatives gives the total number of false results—as compared to the survey group—for a particular threshold.

This sum of false results can therefore be considered a measure of accuracy—as compared to human perception—of a circularity method at a particular threshold. If the number of false results is then calculated for multiple potential thresholds, a graph can be drawn showing the accuracy of the circularity method versus the potential threshold values. Such graphs can be seen in Fig. 9. Three graphs are required because the measures have different empirical ranges.

From these graphs it can be seen that the minimum possible number of false results is lowest for the Radius Ratio, Roundness Factor and Sampled Form Factor, each of which have a minimum of 3 (2.1%) false results out of the 140 categorised cells. The Mean Roundness had a minimum of 4 false results (2.9%); the Circularity Factor a minimum of 6 false results (4.3%); the Fourier Transform Circularity had a minimum of 7 false results (5%) and the Form Factor was worst with a minimum of 15 false results (10.7%).

The graphs for the Circularity Factor and Mean Roundness are noticeable similar. When considering Figs. 4 and 6, the reason becomes obvious: they are using very similar data. They are different only in that the Circularity Factor is based on area difference and the Mean Roundness on radius difference. Since the average radius and the object's area are highly correlated for close-to-round objects, the two measures give similar values the more circular the object. In the portion of the graphs that is not shown—where the objects are least circular—the two measures diverge.

Finally, it is worth noting that the two techniques that use sampling did not reject any of the shapes that human perception deemed circular.

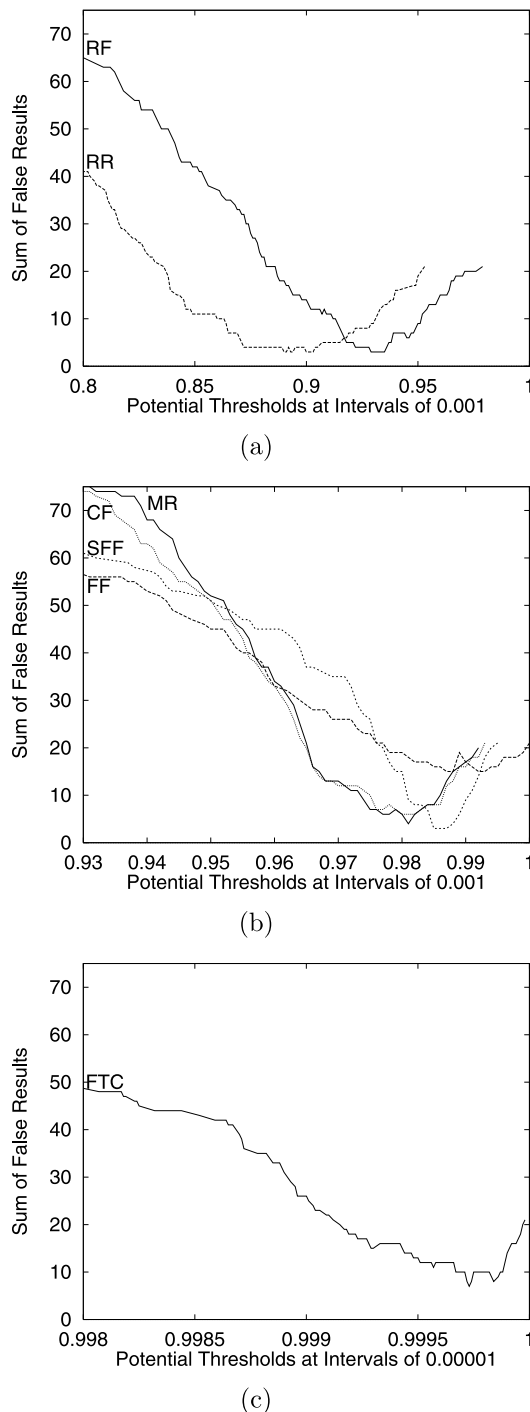


Fig. 9 The sum of false results for the human perception test for the seven different measures for different potential thresholds. Three different graphs are required because the measures have different empirical ranges

5 Conclusion

This paper reviews measures of circularity and demonstrates that most of the measures described in the literature are in fact mathematical derivations of only one, the Form Factor.

Other measures described in the literature that *are* different to this are the Sampled Form Factor, Circularity Factor, Roundness Factor, and Fourier Transform Roundness. The first three of these and the Form Factor all have ranges of $(0..1]$, where only a circle can have a value of 1. However the Fourier Transform Roundness has a theoretical lower bound of 0 for a circle, and we found it to have an empirical upper bound of 1. We therefore define the Fourier Transform Circularity as simply $1 - FFR$ to give it the same range as the other measures.

We have also introduced two new measures. The first of these—the Mean Roundness—is based on the theory of Mean Deviations, and has been normalised to have a theoretical range of $(0..1]$. The second new measure—the Radius Ratio—is based on the definition of a circle and this too has a range of $(0..1]$. Thus there are seven measures that we compare: the Form Factor, Sampled Form Factor, Circularity Factor, Roundness Factor, Fourier Transform Circularity, Mean Roundness and Radius Ratio.

The comparisons done found that the Form Factor—although the most commonly used measure—is the poorest as it is highly resolution dependent, requires identification of both the border and interior points of the object, produced the poorest match with human perception, and has been demonstrated to be a measure of octagonality rather than circularity.

The Roundness Factor and Circularity Factor were also shown to be resolution dependent and they also both require identification of the points interior to the object. The Roundness Factor has the worst complexity of all the measures, however it does have a good match with human perception.

The Sampled Form Factor and the Fourier Transform Circularity both use sampling techniques, which means that they are not defined for all two dimensional shapes. Furthermore, the sampling resulted in some objects having a calculable value at some resolutions and not at others, as well as the rejection of all of the high resolution objects. The Fourier Transform Circularity is also the second slowest measurement to calculate and did not match human perception particularly well.

Both the Mean Roundness and the Radius Ratio were shown to provide resolution independent ordering of the shapes based on the calculated measure. They also both give good matches to human perception, and have $O(n)$ complexity, where n is the number of pixels forming the border. The Radius Ratio, however, should be faster to calculate as each border point is only visited once, not twice.
























































































































In summary, we introduce two new measures of roundness, both of which out-perform previous measures when considering complexity, the data required for calculation, resolution independence and the matching of human perception.

Appendix A: Results for the 18 Digitally-Drawn Shapes

This table shows the calculated values for the seven measures for 18 digitally drawn basic shapes. Results for each measure are sorted to assist comparison. The horizontal lines indicate that the shapes below the line could not be measured using the sampling techniques of the Sampled Form Factor (SFF) or the Fourier Transform Circularity (FTC).

Appendix B: Results for the 6 Hand-Drawn Shapes

This table shows sorted results for the seven measures for 6 hand-drawn shapes—see Fig. 7—that were scanned in at multiple different resolutions. SN is the shape number given in Fig. 7. The shape numbers have coloured backgrounds to make it easier to see the position of the same shape for different resolutions. These results show that the Form Factor is highly resolution dependent and that both of the methods that use sampling reject objects at some resolutions and not at others; the horizontal lines indicate that the shapes below the line could not be measured. It is also worth noting that the Fourier Transform Circularity is the only measure that does not place the hand-drawn circle at the top of the list. The only measures that maintain the relative order of the shapes for different resolutions are the Mean Deviation and the Radius Ratio.

FF	SFF	RF	CF	FTC	MR	RR
 1.050 ^a	 0.995	 0.980	 0.997	 1.000	 0.996	 0.977
 1.000	 0.992	 0.967	 0.987	 1.000 ^b	 0.987	 0.930
 0.995	 0.976	 0.965	 0.987	 1.000	 0.987	 0.927
 0.988	 0.963	 0.950	 0.986	 1.000	 0.980	 0.912
 0.974	 0.942	 0.921	 0.983	 0.999	 0.973	 0.864
 0.928	 0.917	 0.895	 0.982	 0.997	 0.964	 0.856
 0.919	 0.911	 0.892	 0.979	 0.993	 0.948	 0.821
 0.883	 0.820	 0.846	 0.976	 0.980	 0.947	 0.730
 0.864	 0.647	 0.834	 0.973	 0.973	 0.944	 0.688
 0.856	— 0.102	 0.806	 0.963	— 0.704	 0.937	 0.687
 0.845	 -1	 0.704	 0.944	 -1	 0.916	 0.611
 0.774	 -1	 0.646	 0.935	 -1	 0.902	 0.608
 0.725	 -1	 0.634	 0.909	 -1	 0.888	 0.552
 0.622	 -1	 0.607	 0.851	 -1	 0.872	 0.479
 0.548	 -1	 0.532	 0.832	 -1	 0.864	 0.468
 0.378	 -1	 0.508	 0.817	 -1	 0.845	 0.258
 0.274	 -1	 0.330	 0.502	 -1	 0.809	 0.160
— 0.110	 -1	— 0.042	— 0.218	 -1	— 0.695	— 0.033

^aThis value for the Form Factor is greater than one because the perimeter of digitised objects cannot be calculated exactly [38]

^bFive decimal places are required to differentiate between round and almost round objects using the FTC

Form Factor			Sampled Form Factor			Roundness Factor		Circularity Factor		Fourier Transform Circularity			Mean Roundness		Radius Ratio					
Res.			Res.			Res.		Res.		Res.			Res.		Res.					
SN	x100	FF	SN	x100	SFF	SN	x100	RF	SN	x100	CF	SN	x100	FTC	SN	x100	MR	SN	x100	RR
1	1	0.993	1	1	0.994	1	6	0.976	1	8	0.991	3	1	1.000	1	1	0.990	1	4	0.938
5	1	0.984	3	1	0.969	1	3	0.975	1	6	0.990	3	2	1.000	1	2	0.990	1	8	0.937
1	2	0.981	3	3	0.964	1	8	0.974	1	3	0.990	3	3	1.000	1	3	0.990	1	3	0.937
5	2	0.974	3	4	0.964	1	2	0.974	1	4	0.990	3	4	1.000	1	6	0.989	1	6	0.937
1	3	0.970	4	1	0.963	1	4	0.973	1	1	0.990	1	1	1.000	1	4	0.989 ⁺	1	2	0.937
5	3	0.966	4	2	0.963	1	1	0.973	1	2	0.990	4	3	1.000	1	3	0.989	1	1	0.933
4	1	0.963	3	2	0.962	3	6	0.963	3	1	0.989	4	2	1.000	3	8	0.989	3	6	0.932
1	4	0.961	5	3	0.962	3	4	0.962	3	6	0.989	4	1	1.000	3	2	0.989	3	8	0.932
4	2	0.954	5	1	0.961	3	8	0.962	3	4	0.989	5	3	1.000	3	1	0.989	3	1	0.931
4	3	0.947	4	3	0.960	3	3	0.961	3	3	0.989	5	1	1.000	3	4	0.989	3	3	0.930
5	4	0.946	6	4	0.951	3	2	0.960	3	2	0.989	6	3	0.999	3	6	0.988	3	4	0.929
1	6	0.941	6	2	0.951	4	3	0.960	3	8	0.983	6	4	0.999	3	8	0.988	3	2	0.928
4	4	0.940	6	3	0.951	3	1	0.959	4	6	0.983	6	2	0.999	4	8	0.984	5	3	0.891
3	1	0.934	6	1	0.946	4	1	0.959	4	2	0.982	6	1	0.999	4	6	0.984	5	2	0.890
1	8	0.924	2	1	-1	4	4	0.958	4	3	0.982	2	1	-1	4	4	0.983	5	4	0.888
6	1	0.917	1	2	-1	4	6	0.958	4	4	0.982	1	2	-1	4	3	0.983	5	8	0.888
4	6	0.917	2	2	-1	4	2	0.958	4	1	0.982	2	2	-1	4	2	0.982	5	6	0.887
3	2	0.916	5	2	-1	4	8	0.956	5	2	0.980	5	2	-1	4	1	0.981	5	1	0.884
5	6	0.914	1	3	-1	6	4	0.909	5	4	0.980	1	3	-1	5	2	0.980	6	8	0.853
6	2	0.912	2	3	-1	6	6	0.908	5	6	0.980	2	3	-1	5	4	0.980	6	6	0.850
3	3	0.910	1	4	-1	6	8	0.906	5	3	0.980	1	4	-1	5	6	0.980	6	4	0.850
4	8	0.909	2	4	-1	6	3	0.903	5	1	0.979	2	4	-1	5	8	0.980	6	2	0.850
6	3	0.908	4	4	-1	5	2	0.902	5	8	0.976	4	4	-1	5	3	0.980	6	3	0.848
5	8	0.900	5	4	-1	5	6	0.902	4	8	0.966	5	4	-1	5	1	0.980	6	1	0.844
3	4	0.900	6	6	-1	5	1	0.900	6	4	0.966	6	6	-1	6	6	0.967	4	1	0.840
6	4	0.900	1	6	-1	5	4	0.899	6	8	0.966	1	6	-1	6	4	0.967	4	3	0.835
6	6	0.883	2	6	-1	6	2	0.899	6	6	0.966	2	6	-1	6	2	0.967	4	2	0.834
6	8	0.875	3	6	-1	5	3	0.899	6	2	0.966	3	6	-1	6	3	0.967	4	4	0.828
3	6	0.875	4	6	-1	5	8	0.899	6	3	0.966	4	6	-1	6	1	0.967	4	6	0.826
3	8	0.860	5	6	-1	6	1	0.892	6	1	0.966	5	6	-1	6	8	0.967	4	8	0.824
2	1	0.783	6	8	-1	2	1	0.867	2	1	0.955	6	8	-1	2	1	0.958	2	1	0.789
2	2	0.768	1	8	-1	2	6	0.864	2	4	0.954	1	8	-1	2	3	0.958	2	6	0.788
2	3	0.763	2	8	-1	2	3	0.864	2	3	0.954	2	8	-1	2	2	0.958	2	2	0.788
2	4	0.751	3	8	-1	2	4	0.864	2	2	0.954	3	8	-1	2	6	0.957	2	4	0.787
2	6	0.736	4	8	-1	2	8	0.864	2	6	0.954	4	8	-1	2	4	0.957	2	3	0.786
2	8	0.728	5	8	-1	2	2	0.862	2	8	0.953	5	8	-1	2	8	0.957	2	8	0.786

References

- Bacus, J., Belanger, M., Aggarwal, R., Trobaugh, F., Jr.: Image processing for automated erythrocyte classification. *J. Histochem. Cytochem.* **24**(1), 195–201 (1976)
- Bacus, J., Weens, J.: An automated method of differential red blood cell classification with application to the diagnosis of anemia. *J. Histochem. Cytochem.* **25**(7), 614–632 (1977)
- Bacus, J.: Quantative morphological analysis of red blood cells. *Blood Cells* **6**, 295–314 (1980)
- Robinson, R., Benjamin, L., Cosgriff, J., Cox, C., Lapets, O., Rowley, P., Yatco, E., Wheelless, L.: Textural differences between AA and SS blood specimens as detected by image-analysis. *Cytometry* **17**, 167–172 (1994)
- Wheelless, L., Robinson, R., Lapets, O., Cox, C., Rubio, A., Weintraub, M., Benjamin, L.: Classification of red-blood-cells as normal, sickle, or other abnormal, using a single image analysis feature. *Cytometry* **17**, 159–166 (1994)
- Pambuccian, S.E., Becker, R.L., Ali, S.Z., Savik, K., Rosenthal, D.L.: Differential diagnosis of Hürthle cell neoplasms on fine needle aspirates. *Acta Cytol.* **41**, 197–208 (1997)
- Dasgupta, A., Lahiri, P.: Digital indicators for red cell disorder. *Curr. Sci.* **78**, 1250–1255 (2000)
- Foresto, P., D'Arrigo, M., Carreras, L., Cuezso, R., Valverde, J., Rasia, R.: Evaluation of red blood cell aggregation in diabetes by computerized image analysis. *Med. B. Aires* **60**(5), 570–572 (2000)
- LoPachin, R., Jortner, B., Reid, M., Das, S.: Gamma-diketone central neuropathy: quantitative morphometric analysis of axons in rat spinal cord white matter regions and nerve roots. *Toxicol. Appl. Pharmacol.* **193**, 29–46 (2003)
- Mohler, J.L., Partin, A.W., Epstein, J.I., Lohr, W.D., Coffey, D.S.: Nuclear roundness factor measurement for assessment of prog-

- nosis of patients with prostatic carcinoma. ii. standardization of methodology for histologic sections. *J. Urol.* **139**, 1085–1090 (2008)
11. Giger, M., Doi, K., MacMahon, H.: Image feature analysis and computer aided diagnosis in digital radiography. 3. automated detection of nodules in peripheral lung fields. *Med. Phys.* **15**(2) (1988)
 12. Artacho-Pérula, E., Roldán-Villalobos, R., Martínez-Cuevas, J.F., López-Rubio, F.: Nuclear quantitative grading by discriminant analysis of renal cell carcinoma samples. a patient survival evaluation. *J. Parasitol.* **173**, 105–114 (1994)
 13. Landry, M.E., Blanchard, C.R., Mabrey, J.D., Wang, X., Agrawal, C.M.: Morphology of in vitro generated ultrahigh molecular weight polyethylene wear particles as a function of contact conditions and material parameters. *J. Biomed. Mater. Res. Part B, Appl. Biomater.* **48**(1), 61–69 (1999)
 14. Breslow, N., Partin, A., Lee, B., Guthrie, K., Beckwith, J., Green, D.: Nuclear morphometry and prognosis in favorable histology Wilms' tumor: A prospective reevaluation. *J. Clin. Oncol.* **17**, 2123–2126 (1999)
 15. Gordon, A., Cloman-Lerner, A., Chin, T.E., Benjamin, K., Yu, R.C., Brent, R.: Supplementary notes to: Single-cell quantification of molecules and rates using open-source microscope-based cytometry. *Nat. Methods* **4**(2) (2007), p. 22 of the supplement
 16. Nikolakakis, I., Kachrimanis, K., Malamataris, S.: Relations between crystallisation conditions and micromeritic properties of ibuprofen. *Int. J. Pharm.* **201**, 79–88 (2000)
 17. Cenens, C., Jenne, R., Impe, J.V.: Evaluation of different shape parameters to distinguish between flocs and filaments in activated sludge images. *Water Sci. Technol.* **45**(45), 85–91 (2002)
 18. Almeida-Prieto, S., Blanco-Mendez, J., Otero-Espinar, F.: Image analysis of the shape of granulated powder grains. *J. Pharm. Sci.* **93**, 621–634 (2004)
 19. Jayaraj, J., Fleury, E., Kim, K., Lee, J.: Globulization mechanism of the primary Al of Al-15Cu alloy during slurry preparation for rheofforming. *Met. Mater. Int.* **11**, 257–262 (2005)
 20. Moschakis, T., Murray, B., Dickinson, E.: Microstructural evolution of viscoelastic emulsions stabilised by sodium caseinate and xanthan gum. *J. Colloid Interface Sci.* **284**, 714–728 (2005)
 21. Clemens, J., Henriod, R., Bailey, D., Jameson, P.: Vegetative phase change in metrosideros: Shoot and root restriction. *Plant Growth Regul.* **28**, 207–214 (1999)
 22. Dell'Aquila, A.: Cabbage, lentil, pepper and tomato seed germination monitored by an image analysis system. *Seed Sci. Technol.* **32**(1), 225–229 (2004)
 23. Gardoll, S., Groves, D., Knox-Robinson, C., Yun, G., Elliott, N.: Developing the tools for geological shape analysis, with regional-to local-scale examples from the Kalgoorlie Terrane of Western Australia. *Aust. J. Earth Sci.* **47**, 943–953 (2000)
 24. Kanthathas, K., Willmot, D., Benson, P.: Differentiation of developmental and post-orthodontic white lesions using image analysis. *Eur. J. Orthod.* **27**, 167–172 (2005)
 25. Huff, P., Wilf, P., Azumah, E.: Digital future for paleoclimate estimation from fossil leaves? Preliminary results. *Palaaios* **18**, 266–274 (2003)
 26. Springham, S., Lee, S., Moo, S.: Deuterium plasma focus measurements using solid state nuclear track detectors. *Braz. J. Phys.* **32**, 172–178 (2002)
 27. Cox, E.: A method of assigning numerical and percentage values to the degree of roundness of sand grains. *J. Paleontol.* **1**(3), 179–183 (1927)
 28. Nafe, R., Yan, B., Schlote, W., Schneider, B.: Application of different methods for nuclear shape analysis with special reference to the differentiation of brain tumors. *Anal. Quant. Cytol. Histol.* **28**, 69–77 (2006)
 29. Payne, C., Bjore, C., Jr., Cromley, D., Roland, F.: A comparative mathematical evaluation of contour irregularity using form factor and PERBAS, a new analytical shape factor. *Anal. Quant. Cytol. Histol.* **11**, 341–352 (1989)
 30. Bouwman, A., Bosma, J., Vonk, P., Wesselingh, J., Frijlink, H.: Which shape factor(s) best describe granules? *Powder Technol.* **146**, 66–72 (2004)
 31. Shen, H.: Regular form factor—a new concept and calculating method for quantitative form description. *Anal. Quant. Cytol. Histol.* **22**, 453–458 (2000)
 32. The American Society for Testing and Materials, Standard practice for characterization of particles (2005)
 33. Richardson, L.F.: The problem of contiguity: An appendix to statistics of deadly quarrels. *Gen. Syst. Yearbook* **6**, 139–190 (1961)
 34. Hausner, H.H.: Characterization of the powder particle shape. *Planseeber. Pulvermetall.* **14**, 75–84 (1966)
 35. Blanco, A., Tomasi, F.D., Filippo, E., Manno, D., Perrone, M., Serra, A., Tafuro, A., Tepore, A.: Characterization of African dust over southern Italy. *Atmos. Chem. Phys.* **3**, 2147–2159 (2003)
 36. Diamond, D.A., Berry, S.J., Jewett, H.J., Eggleston, J.C., Coffey, D.S.: A new method to assess metastatic potential of human prostate cancer: Relative nuclear roundness. *J. Urol.* **128**, 729–734 (1982)
 37. Mandelbrot, B.: How long is the coast of Britain? statistical self-similarity and fractional dimension. *Science* **156**, 636–638 (1967)
 38. Dorst, L., Smeulders, A.: Length estimators for digitized contours. *Comput. Vis. Graph. Image Process.* **40**, 311–333 (1987)
 39. Bottema, M.: Circularity of objects in images. In: Proceedings of the IEEE International Conference on Acoustics, Speech, and Signal Processing (ICASSP '00'), pp. 2247–2250. IEEE Press, New York (2000)
 40. Hawkins, A.E.: The shape of powder-particle outlines. *Meas. Sci. Technol.*, vol. 1 (1993)
 41. Pentland, A.: A method of measuring the angularity of sands. In: Proceedings & Transactions of the Royal Society of Canada, vol. 21 (1927)
 42. Toussaint, G.T.: Rotating calipers. Aug. 2006. <http://www-cgrl.cs.mcgill.ca/%7Egodfried/research/calipers.html>
 43. Sunday, D.: The convex hull of a 2d point set or polygon. Aug. 2006. http://www.geometryalgorithms.com/Archive/algorithm_0109/algorithm_0109.htm
 44. Ritter, N., Cooper, J.R.: Segmentation and border identification of cells in images of peripheral blood smear slides. In: Thirtieth Australasian Computer Science Conference (ACSC2007). Ballarat Australia, pp. 161–169. ACS, Washington (2007)